Review of MS. MS No.: EGUSPHERE-2025-6531
Title: Estimation of Nocturnal Boundary Layer Height in the Central Amazon, Supported by Gas Concentration Profiles

Response (blue color) to anonymous **Referee #2** (black). The original manuscript was changed accordingly. Please note that all line numbers indicated in our responses refer to the tracked-changes version of the revised manuscript.

General comments

This manuscript by Carla Souza et al. investigates the height of the nocturnal boundary layer (hn) above the central Amazon using micrometeorological observations from the Amazon Tall Tower Observatory. By analyzing vertical profiles of turbulent sensible heat flux up to 300 m, the authors estimate hn more directly than many previous studies that rely on indirect proxies. The analysis focuses on seasonal differences between wet and dry periods during one La Ni˜na year and one El Ni˜no year. The authors report substantial variability in nocturnal boundary layer height, with the largest values occurring during the wet season of the La Niña year (approximately 270 ± 40 m) and the smallest during the dry season associated with El Ni˜no (approximately 100 ± 27 m). They further show that variations in hn influence the vertical distribution of CO and CH4, with the boundary layer height acting as a barrier that can limit the exchange of air masses containing elevated trace gas concentrations. Overall, the study provides observational evidence of strong seasonal and interannual variability in the nocturnal boundary layer over the Amazon and highlights implications for the representation of boundary layer processes and trace-gas transport in atmospheric models.

The manuscript addresses an interesting and relevant topic; however, substantial revisions are required before it can be considered for publication. In its current form, the study would benefit from more in-depth investigation of the underlying physics and in-canopy processes. The analysis appears somewhat limited, and important mechanisms are not sufficiently explored or supported. Additionally, the manuscript is relatively short for a full paper, and several limitations of the study are not adequately discussed. Expanding on these aspects would improve the rigor and clarity of the work. While I find some of the ideas promising and appreciate the effort, there are a number of significant points that must be clarified. I would like to see detailed responses to the comments provided below, as they are essential for properly evaluating the study.

Given the scope and depth of the current manuscript, I suggest that the work may be more suitable for consideration as a letter rather than a full research article. Below are my specific comments:

We thank Reviewer #2 for the careful evaluation of our manuscript and for the constructive comments. We appreciate the reviewer's positive assessment of the relevance of the topic and of our observational approach to estimate the nocturnal boundary-layer height from vertical profiles of turbulent sensible heat flux.

Following the reviewer's suggestions, we have revised the manuscript to strengthen the physical interpretation of the results and to better discuss the mechanisms controlling hn. In particular, we expanded the discussion of thermal stability, turbulence, wind shear, radiative cooling, seasonal/interannual variability, and their implications for trace-gas transport. We also added supporting analyses and clarified the limitations of the study. Regarding the suggestion that the manuscript may be more suitable as a letter, we respectfully believe that the revised version is now appropriate as a full research article.

All comments have been addressed below, and the manuscript has been revised accordingly.

Specific comments

• Lines 24-25: Attribute the reported differences of zi between pastures and forests patches to the physical implications. It is also useful to define how zi is calculated in the literature

We agree with the reviewer and updated the text in the revised manuscript as detailed below:

L26-30: " estimated zi from radiosonde data as the height of the main inversion layer, identified from the vertical profile of potential temperature. They showed that zi values differ between pasture and forest areas, with a deeper boundary layer over pasture, up to ~1650 m, compared to forest, ~1100 m. This contrast is attributed to differences in surface energy partitioning, since pasture areas exhibit higher sensible heat fluxes and lower evapotranspiration compared to forests, leading to stronger thermal turbulence and enhanced boundary layer growth."

• Line 35: zi and not Zi

Thank you for pointing this out. This has been corrected in the revised manuscript (L39).

• Line 61: Again, mention how Mendonça et al. defined the calculation of zi

We clarified this point in the revised manuscript by rephrasing the sentence as follows:

L60-61: "These estimates are based on the height at which H falls below 5% of its near-surface value."

• Line 82: Define the air temperature variable symbol (T).

Thank you for pointing this out. This has been corrected in the revised manuscript (L89).

• Line 94: Is 30-min your Reynolds average? Any double rotation of the wind is attempted? Linear detrending?

We thank the reviewer for this question. The 30-minute subsets (18000 records) were not used as Reynolds averaging intervals, but for quality control (QC) procedures following Vickers and Mahrt (1997) and Zahn et al. (2016), including checks of data completeness, identification of error flags, spike detection and removal, and stationarity tests. After QC, the planar fit method (Wilczak et al., 2001) was used for tilt correction. For each six-month period, wind velocity components were used to estimate the anemometer tilt angles and define a mean streamline coordinate system. The tilt-corrected wind vectors were then rotated for each 30-min interval to align the horizontal wind component with the mean wind direction (Kaimal & Finnigan, 1994). Subsequently, linear detrending was applied to 5-minute time windows, within which turbulent fluctuations and statistics were calculated.

The following sentence has been updated to the revised manuscript:

L105-118: "As in other micrometeorological studies (Foken and Mauder, 2008; Starkenburg et al., 2016; Dias et al., 2023), the high frequency data were initially segmented into 30-minute intervals (totaling 18000 measurements) for the application of quality control (QC) procedures and tilt correction. QC was performed for each wind component and for the temperature measured by the sonic anemometers. The QC process included verification of record integrity, detection of error indicators, identification and removal of spikes, as well as the application of stationarity tests. For a detailed description of the quality control protocol adopted at the ATTO Site, it is recommended to consult Zahn et al. (2016) and Dias et al. (2023).

After QC, the planar fit method (Wilczak et al., 2001) was used for tilt correction. For each six-month period, wind velocity components were used to estimate the anemometer tilt angles and define a mean streamline coordinate system. The tilt-corrected wind vectors were then rotated for each 30-min interval to align the horizontal wind components with the mean wind direction (Kaimal and Finnigan, 1994). Subsequently, turbulence statistics were calculated over 5-minute windows using Reynolds averaging, after applying linear detrending within each window. This shorter time window reduces the influence of non-turbulent motions, which are relevant under stable boundary layer conditions (Sun et al., 2002; Oliveira et al., 2018)."

• Line 100: 5-min turbulence statistics. clarify how does it differ from the above 30-min Reynolds average? Delineate clearly between QC and Reynolds averaging. Justify these choices.

We thank the reviewer for these points. As clarified above, 30-minute blocks were used exclusively for QC procedures, whereas turbulence statistics were computed over 5-minute windows. This choice was made to better capture turbulent fluctuations while minimizing contamination from non-turbulent motions, which are relevant under stable boundary layer conditions (Sun et al., 2002; Oliveira et al., 2018). We have incorporated these clarifications into the revised manuscript, as detailed in our response to the previous comment (L101-L117 this document).

• Line 116: Justify these thresholds and the sensitivity to these thresholds.

We thank the reviewer for the opportunity to clarify this point. The filtering thresholds were defined from the observed distribution of sensible heat flux (H) at each height range, while accounting for the expected decrease in flux magnitude with height above the canopy.

To test the sensitivity of hn to these thresholds, we applied two additional filtering scenarios. The baseline thresholds were −50 to 0 Wm^{-2} for 50–81 m, −30 to 10 Wm^{-2} for 100–151 m, and −20 to 10 Wm^{-2} for 172–298 m (Scenario 3). The permissive scenario expanded these ranges to −60 to 20, −45 to 25, and −35 to 15 Wm^{-2} (Scenario 2) respectively. The restrictive scenario reduced them to −30 to 0, −20 to 5, and −10 to 5 Wm^{-2} (Scenario 1), respectively.

The sensitivity test shows that the normalized heat-flux profiles and the estimated hn are very similar across the three scenarios (Figure 1). The difference in estimated hn was less than 15 m. This indicates that the main results are robust and not sensitive to the specific filtering thresholds used.

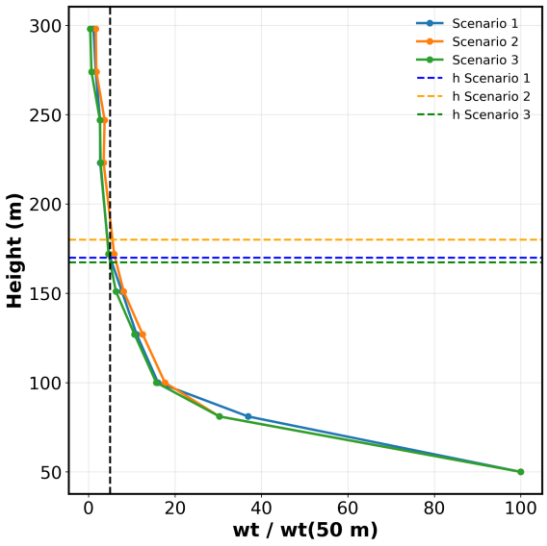

Figure 1. (Figure S1 in the new version of the manuscript) Sensitivity analysis of the filtering thresholds applied to the sensible heat flux (H). The normalized profiles (H/H50×100) are shown for three scenarios: the original thresholds (−50 to 0 W m−2 for 50–81 m, −30 to 10 W m−2 for 100–151 m, and −20 to 10 Wm−2 for172–298 m;Scenario 3), a more permissive scenario (−60 to 20, −45 to 25, and −35 to 15 W m−2; Scenario 2), and a morerestrictive scenario (−30 to 0, −20 to 5, and −10 to 5 Wm−2; Scenario 1). Dashed horizontal lines indicate the corresponding hn values.

We added this justification and the sensitivity analysis to the revised manuscript and included the figure in the Supplementary Material.

L 136-140: “To test the sensitivity of hn to these filtering limits, we applied a more permissive scenario (−60 to 20, −45 to 25, and −35 to 15 W m−2; Scenario 2) and a more restrictive scenario (−30 to 0, −20 to 5, and −10 to 5 W m−2; Scenario 1) for the three height ranges. The normalized profiles were very similar, and the estimated hn differed by less than 15 m among scenarios (Fig. S1), indicating that the results are robust to the selected thresholds.”

• Line 142: There is another definition of hn as the height at which TKE drops below a certain percentage of the measured TKE near the surface. Why this criterion is not adopted ? Also, how would the results change based on the latter? In this context and since TKE friction velocity a measure of the shear strength, did you look at Richardson number that shows the competition between buoyancy and shear?

We appreciate the reviewer’s suggestion. Indeed, both the sensible heat flux (H) and the turbulent kinetic energy (TKE) can be used to characterize turbulence. The H decreases with height and approaches zero at the level where turbulent mixing is suppressed, providing a direct indication of the NBL top (Fig. 2a). In contrast, although TKE also decreases with height, it does not become negligible at the NBL top (Fig. 2b), because non-turbulent motions can still contribute to velocity variances above this level (Acevedo et al., 2016).

This limitation has already been evaluated for the ATTO site. Huitema et al. (2026), analyzing observations during the dry season of 2022, estimated hn using different approaches and compared them against a reference hn derived from potential temperature profiles. Using a TKE-based criterion defined as the height where TKE is reduced to 20% of its canopy-top value, they found that this approach overestimates hn by approximately 18%. In addition, a Richardson number (Ri)-based criterion, defined as the lowest level where Ri ≥ 0.25, underestimates hn by approximately 19% (their Fig. 2). For this reason, we adopt H as the primary criterion, as it better represents the upper limit of turbulent mixing in the NBL.

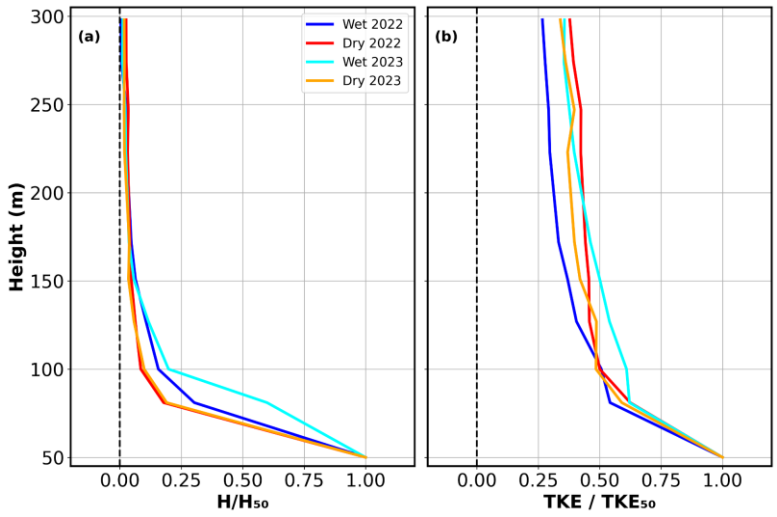

Figure 2. Average vertical profiles of normalized a) sensible heat flux (H) and b) turbulent kinetic energy (TKE) for wet and dry seasons in 2022 and 2023.

• Line 159: Report the value ζ = z/L

We thank the reviewer. In the revised manuscript, we have included quantitative values of the (z/L)

L184: “The Wet period is less stable (smaller z/L = 2.15), while the Dry period shows stronger stability (z/L = 3.10).”

• Line 163: After looking at figure 3, the results look so sensitive to the choice of 5%! Without loss of generality, if you opted to choose 6% for example, the reported values would drastically change. Any thoughts?

We thank the reviewer for the opportunity to clarify the 5% threshold used to estimate hn. The choice of the 5% threshold was based on previous studies (i.e. Nieuwstadt, 1984; Lenschow et al., 1988) since it reflects a point where turbulence, although still present, has significantly diminished relative to surface values (Stull 1988; Kaimal & Finnigan, 1994). Furthermore, this threshold offers a standardized method for defining hn, facilitating comparisons across different regions. Figure 3 of this document shows a normalized vertical profile of the sensible heat flux ($\overline{w'T'}$) using the flux value at 50 m as the reference (100%). The percentages on the x-axis represent the relative contribution of $\overline{w'T'}$ at each height compared to 50 m. The results demonstrate that hn estimates using the 3%, 5%, and 7% thresholds vary by less than 30 meters highlighting the robustness of the method.

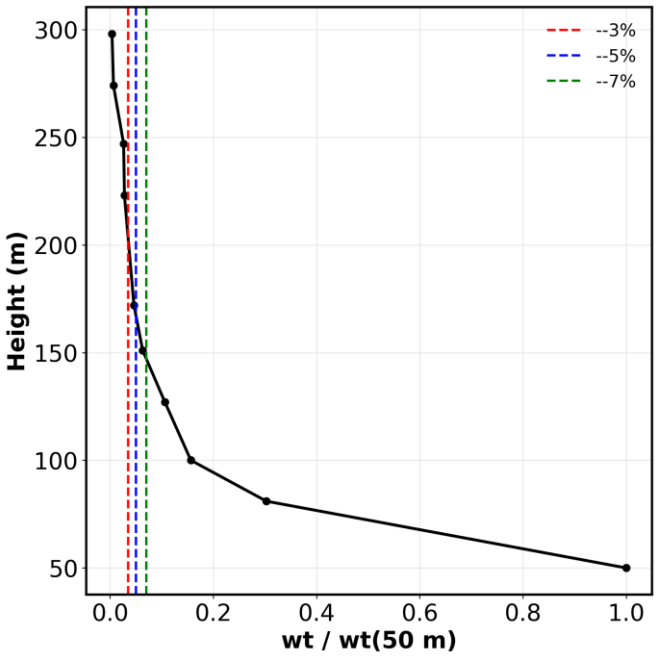

Figure 3. Normalized vertical profile of the sensible heat flux ($\overline{w'T'}$). The dashed vertical lines indicate thresholds at 3% (red), 5% (blue), and 7% (green) of the flux.

• Line 175: Compute the shear and relate to ζ = z/L

We thank Reviewer #2 for this comment. The atmospheric stability parameter (ζ = z/L) was already included in the Supplementary Material (Figure S1 of the previous version of the manuscript), showing the hourly mean evolution of atmospheric stability during the wet and

dry seasons for both years analyzed. As shown in Figure S1, larger ζ = z/L values were associated with stronger atmospheric stability and shallower NBL, particularly during the dry season.

In addition, we expanded the analysis of the two case-study nights, including net radiation (Rn) at 81 m, cloud fraction (%), vertical profile of the potential temperature (θ) difference relative to 298 m, and vertical wind shear (dU/dz) for 18 and 25 August 2022 (Figure 4). To compute wind shear, third-order polynomial fits were applied to the wind speed profiles (U(z)), from which analytical vertical derivatives were calculated. Cloud fraction was estimated from observations obtained by the Cloud Radar Profiler (METEK MIRA-35C) installed at the ATTO site. GOES-16 IR Channel 13 (10.3 µm) brightness temperature imagery was additionally used to illustrate cloud cover conditions during the two nights (Figures 5 and 6).

The night of 18 August 2022 represents a strongly stratified and more decoupled case compared to 25 August 2022. Strong radiative cooling (Fig. 4a), reduced cloud occurrence (Fig. 4c and Fig. 5), and a pronounced vertical potential temperature gradient (Fig. 4e), were associated with a shallow hn, mostly around 80–100 m. Despite the presence of wind shear at some levels, the strong stratification suggests that mechanically generated turbulence aloft was not efficiently coupled downward to the layer near the canopy. This behavior is consistent with a layered nocturnal structure in which the shallow surface-based layer remains isolated from the air above, similar to the regime described by Mahrt and Acevedo (2023). In contrast, the night of 25 August 2022 showed larger cloud cover (Fig. 4d and Fig. 6), reduced radiative cooling during the early night (Fig. 4b), and weaker thermal stratification (Fig. 4f). Wind shear extended to higher levels (Fig. 4h), reaching approximately 150-170 m, close to hn. This suggests that mechanical forcing contributed to sustaining turbulence over a deeper layer under weaker stratification. Therefore, the differences between the two nights are interpreted as the result of the balance between radiative cooling, which enhances stratification and suppresses turbulence, and shear-generated mechanical turbulence, which can deepen or sustain the NBL when coupling is possible.

We included this new analysis in Section 3.3 of the Results and in the new Section 4 (Discussion) of the revised manuscript.

L239–253: “To better identify the main drivers controlling the contrasting hn behavior during the two case-study nights, we further analyzed Rn at 81m, cloud cover,the vertical profile of θ and windshear (dU/dz) (Fig. 9). These variables provide complementary information on the local radiative forcing, cloud modulation of nocturnal cooling, thermal stratification, and mechanical turbulence generation. The night of 18 August 2022 was characterized by strong nocturnal radiative cooling (Fig. 9a), reduced cloud occurrence (Fig. 9c and Fig. S2), and a pronounced vertical potential temperature gradient (Figure 9e). These conditions indicate enhanced thermal stratification near the surface. Although wind shear was observed at some levels (Fig. 9g), the strong stratification suggests that mechanically generated turbulence aloft was not efficiently coupled downward toward the canopy. This supports the interpretation that the shallow hn observed on 18 August 2022 reflects not only strong thermal stratification, but also canopy-induced suppression of vertical mixing near the forest top. This configuration is consistent with a shallow surface-based nocturnal layer that remained partly decoupled from the air above, similar to the layered nocturnal structure described by Mahrt and Acevedo (2023). In contrast, the night of 25 August 2022 showed larger cloud cover (Fig. 9d and Fig.S3), weaker radiative cooling during the early part of the night (Fig. 9b), and weaker thermal stratification (Fig. 9f). Wind shear extended to higher levels (Fig. 9h), reaching approximately 150–170 m, close to the observed hn. This suggests that, under weaker stratification, mechanically generated turbulence was more effectively coupled over a deeper layer, contributing to the larger and more variable hn observed during this night.”

L289-322: “The results presented here demonstrate that the nocturnal boundary-layer height (hn) above the central Amazon is strongly controlled by the interaction between nocturnal radiative cooling, atmospheric stability, cloud cover, and mechanically generated turbulence. Although previous Amazonian studies have primarily focused on the daytime evolution of the atmospheric boundary layer (Fisch et al., 2004; Carneiro and Fisch, 2020; Dias-Júnior et al., 2022), our results show that the nocturnal boundary layer also exhibits pronounced seasonal and interannual variability, with important implications for turbulence exchange and trace-gas transport above tropical forests.

One of the clearest patterns observed in this study is the systematic reduction of hn during the Dry season and during the El Niño year (2023). These periods were characterized by stronger nocturnal net radiative loss (Figure 2a) and enhanced atmospheric stability, reflected by larger z/L values (Figure 2b) and a stronger thermal gradient (Fig. S6b, d). Under these conditions, turbulent exchange becomes increasingly suppressed, limiting the upward transport of sensible heat and favoring the formation of shallower nocturnal layers (Figures 4d and 5b). In contrast, wetter conditions, particularly during the Wet season of 2022, were associated with weaker radiative cooling (Figure 2a), reduced stability (Figure 2b), Weak thermal gradient(Fig S6a, c), and deeper nocturnal layers (Figures 4a and 5a). These findings reinforce the strong coupling between cloud cover, nocturnal cooling, and turbulence generation over the Amazon rainforest.

The hourly evolution of hn also reveals the importance of the temporal evolution of thermal stratification during the night. In all analyzed periods, hn was generally larger at the beginning of the night and progressively decreased toward the early morning hours (Figure 5). This behavior is particularly evident during the Wet season of 2022, when the thermal gradient remained relatively weak during the first hours of the night (Figures 9e,f and S6a), allowing mechanically generated turbulence to sustain a deeper nocturnal boundary layer. As the night progressed, radiative cooling intensified the thermal gradients, suppressing turbulence and leading to a gradual collapse of hn. This progressive reduction of turbulent mixing throughout the night is consistent with the classical evolution of stable nocturnal boundary layers described in previous studies (Mahrt, 1999; Sun et al., 2002).

The results also demonstrate that the interaction between thermal stratification and mechanically generated turbulence is fundamental for understanding the nocturnal boundary-layer structure above the Amazon forest (Figure 9). The case studies revealed that low-level jets (LLJs) (Figure 7) and enhanced vertical wind shear (Figure 9 g,h) may sustain turbulence above the canopy, but the influence of this turbulence on the lower nocturnal boundary layer depends on the degree of vertical coupling between atmospheric layers. This interpretation is consistent with the conceptual framework proposed by Mahrt and Acevedo (2023), in which nocturnal boundary layers may deviate from a vertically monotonic structure and instead exhibit layered configurations composed of shallow surface-based layers, transition layers, and elevated turbulent regions.

Our observations suggest that the forest canopy plays a key role in reinforcing this layered structure. Under strongly stable conditions, the canopy acts as a roughness and drag layer that attenuates momentum transfer toward the surface. Consequently, turbulence generated aloft by LLJs or strong wind shear may remain confined to elevated layers and may not efficiently penetrate downward through the canopy layer. This mechanism likely explains the shallow hn observed on 18 August 2022, when strong thermal stratification and weak vertical coupling produced a highly decoupled nocturnal structure. In contrast, on 25 August 2022, weaker thermal stratification allowed mechanically generated turbulence to penetrate deeper into the lower nocturnal boundary layer, resulting in larger and more vertically connected hn values.”

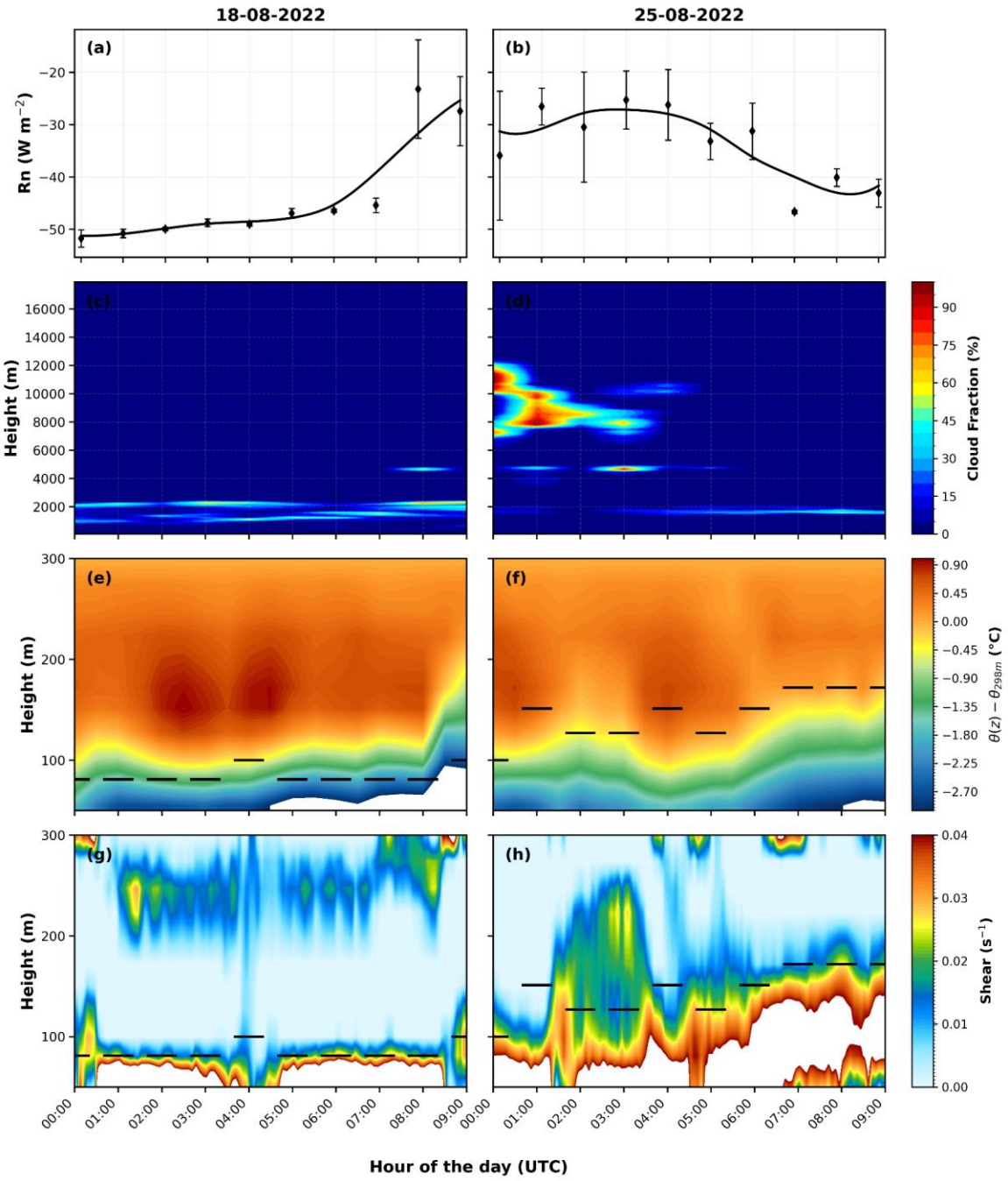

Figure 4 (Figure 9 in new version of the manuscript). Nocturnal evolution of (a, b) hourly mean net radiation (Rn) at 81 m (± standard deviation), (c, d) cloud fraction (%), (e, f) vertical potential temperature (θ) difference from the value observed at 298 m, and (g, h) vertical wind shear (dU/dz) during the case-study nights of 18 August 2022 (left panels) and 25 August 2022 (right panels). Black horizontal segments indicate the estimated nocturnal boundary layer height at each hour.

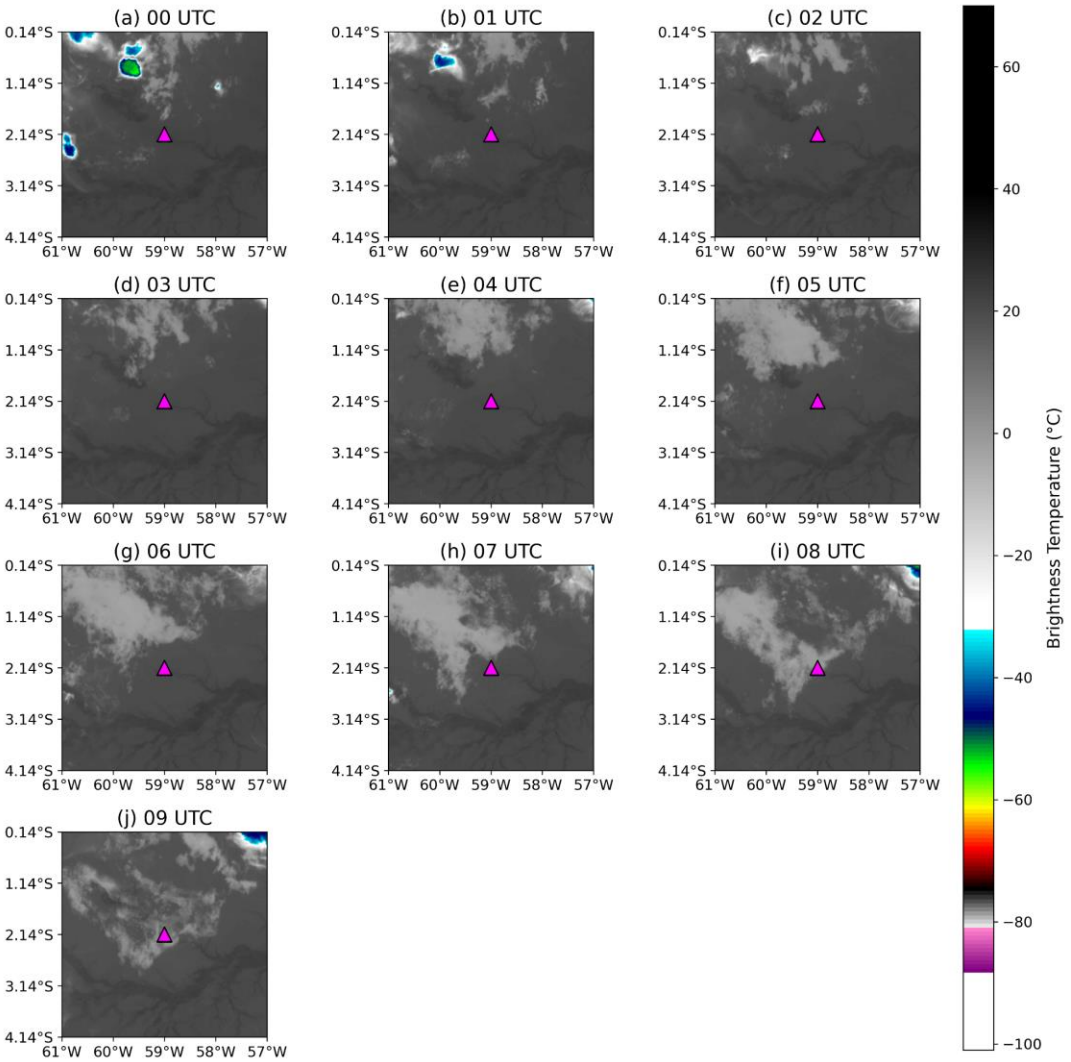

Figure 5 (Figure S2 in new version of the manuscript). GOES-16 IR Channel 13 (10.3 µm) brightness temperature over the ATTO site on 18 August 2022. Panels (a–j) show hourly images from 00 to 09 UTC. The magenta triangle marks the location of the ATTO tower.

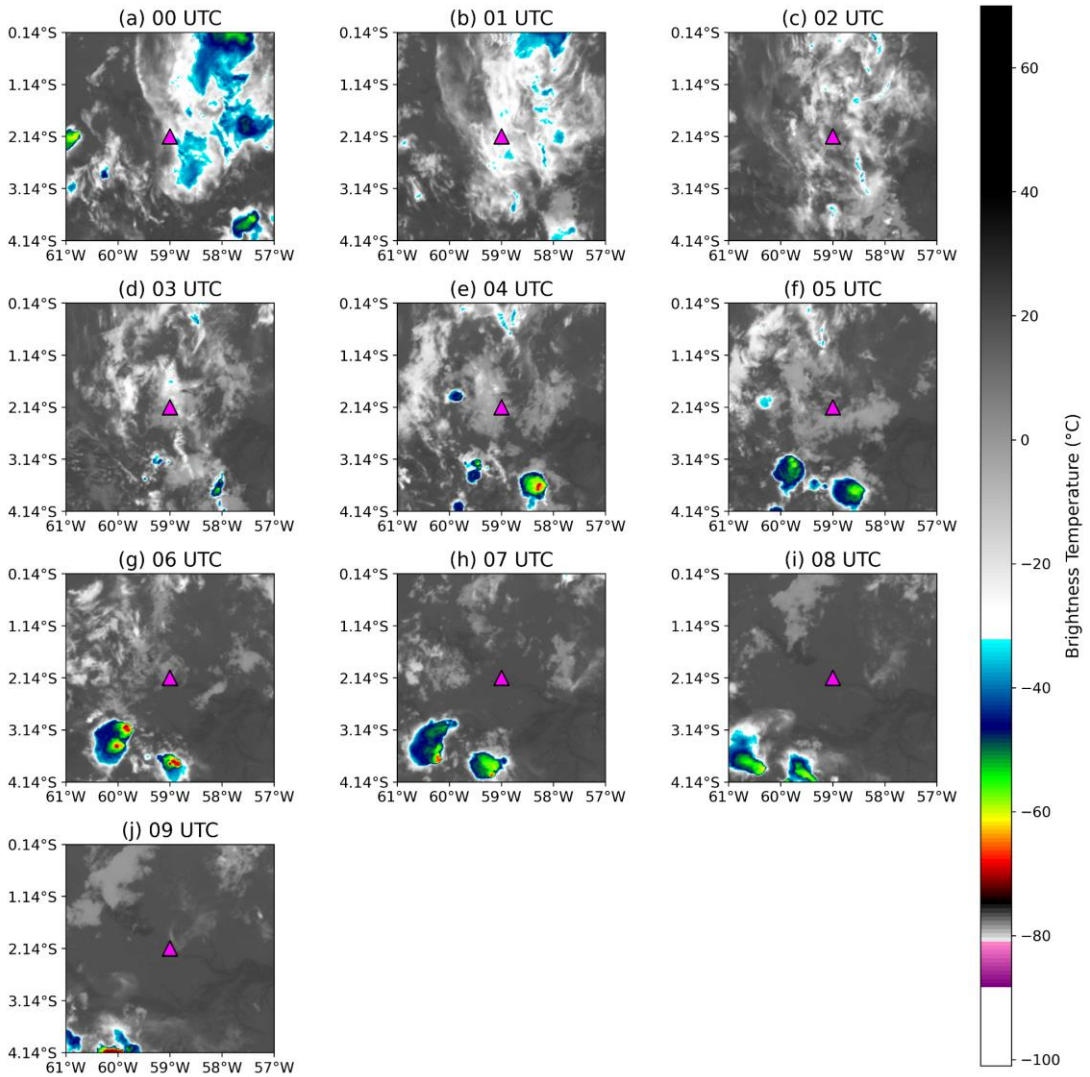

Figure 6 (Figure S3 in new version of the manuscript). GOES-16 IR Channel 13 (10.3 µm) brightness temperature over the ATTO site on 25 August 2022. Panels (a–j) show hourly images from 00 to 09 UTC. The magenta triangle marks the location of the ATTO tower.

• Lines 178-184: The authors attribute the differences in nocturnal radiative loss and boundary-layer structure primarily to variations in cloud cover (e.g., “greater cloud cover results in greater turbulent activity”). While this mechanism is physically plausible from a boundary-layer meteorology perspective, the manuscript does not present a direct metric of cloud cover to support this interpretation. The analysis appears to rely on radiation measurements (e.g., net radiation, Rn), which can indeed reflect differences in radiative cooling but do not uniquely indicate cloudiness. I therefore suggest that the authors either (i) provide additional evidence linking the radiation differences to cloud cover (e.g., through analysis of longwave radiation or another proxy for cloudiness), or (ii) rephrase the discussion more cautiously, framing cloud cover as one possible explanation for the observed radiative differences rather than a demonstrated cause.

We thank Reviewer #2 for this comment. We expanded the analysis of the two case-study nights, as described in the response to the previous comment (Line 258-349 in this document). These additional observations indicate lower (higher) cloud occurrence on 18 August 2022 (25 August 2022), consistent with the observed differences in net radiation between the two cases.

• Line 185: Mention briefly these methods

This clarification has been incorporated into the new discussion section of the revised manuscript as follows:

L345-347: “Most previous studies relied on indirect methods based on thermodynamic profiles, Richardson number, or remote sensing approaches (Santos et al., 2007; Dias-Júnior et al., 2022; Carneiro et al., 2025).”

• Line 186: Based on which method?

This was already solved in prévios comment (Line 78-79 in this document).

• Figure 8 does not differentiate between the 2 selected dates (add respectively in the caption).

We thank the reviewer for this suggestion. Figure 8 has been revised to include the respective dates in the figure titles and captions.

References:

Carneiro, R., Fisch, G., Neves, T., Santos, R., Santos, C., and Borges, C.: Nocturnal boundary layer erosion analysis in the Amazon using large-eddy simulation during GoAmazon project 2014/5, Atmosphere, 12, 240, 2021

Dias-Júnior, C. Q., Carneiro, R. G., Fisch, G., D’Oliveira, F. A. F., Sörgel, M., Botía, S., Machado, L. A. T., Wolff, S., Santos, R. M. N. d., and Pöhlker, C.: Intercomparison of planetary boundary layer heights using remote sensing retrievals and ERA5 reanalysis over Central Amazonia, Remote Sensing, 14, 4561, 2022.

Dias, N. L., Toro, I. M. C., Dias-Júnior, C. Q., Mortarini, L., and Brondani, D.: The relaxed eddy accumulation method over the amazon forest: the importance of flux strength on individual and aggregated flux estimates, Boundary-Layer Meteorology, 189, 139–161, 2023.

Fisch, G., Tota, J., Machado, L., Silva Dias, M. A. F. d., Da F. Lyra, R., Nobre, C., Dolman, A., and Gash, J.: The convective boundary layer over pasture and forest in Amazonia, Theoretical and Applied Climatology, 78, 47–59, 2004

Foken, T., & Mauder, M. (2008). *Micrometeorology* (Vol. 2, p. 306). Berlin: Springer.

Huitema, A. C., de Feiter, V. S., González-Armas, R., Hartogensis, O. K., van Asperen, H., Quaresma Dias-Júnior, C., & Vilà-Guerau de Arellano, J. (2026). CO 2 and Heat exchange across the Nocturnal Canopy–Atmosphere interface in the Amazon rainforest. *EGUsphere*, *2026*, 1-32.

Kaimal, Jagadish Chandran; FINNIGAN, John J. Atmospheric boundary layer flows: their structure and measurement. Oxford university press, 1994.

Lenschow, D. H., Li, X. S., Zhu, C. J., and Stankov, B. B.: The stably stratified boundary layer over the Great Plains: I. Mean and turbulence structure, Boundary-layer meteorology, 42, 95–121, 1988

Mendonça, A. C., Dias-Junior, C. Q., Acevedo, O. C., Marra, D. M., Cely-Toro, I. M., Fisch, G., Brondani, D. V., Manzi, A. O., Portela, B. T., Quesada, C. A., et al.: Estimation of the nocturnal boundary layer height over the Central Amazon forest using turbulence measurements, Agricultural and Forest Meteorology, 367, 110469, 2025

Nieuwstadt, Frans TM. The turbulent structure of the stable, nocturnal boundary layer. Journal of Atmospheric Sciences, v. 41, n. 14, p. 2202-2216, 1984.

Oliveira, P. E., Acevedo, O. C., Sörgel, M., Tsokankunku, A., Wolff, S., Araújo, A. C., ... & Andreae, M. O. (2018). Nighttime wind and scalar variability within and above an Amazonian canopy. *Atmospheric Chemistry and Physics*, *18*(5), 3083-3099.

Starkenburg, D., Metzger, S., Fochesatto, G. J., Alfieri, J. G., Gens, R., Prakash, A., and Cristóbal, J.: Assessment of despiking methods for turbulence data in micrometeorology, Journal of Atmospheric and Oceanic Technology, 33, 2001–2013, 2016

Stull, R. B. (1988). Mean boundary layer characteristics. In *An introduction to boundary layer meteorology* (pp. 1-27). Dordrecht: Springer Netherlands.

Sun, J., Burns, S. P., Lenschow, D. H., Banta, R., Newsom, R., Coulter, R., ... & Hu, X. Z. (2002). Intermittent turbulence associated with a density current passage in the stable boundary layer. *Boundary-Layer Meteorology*, *105*(2), 199-219.

Vickers, D. and Mahrt, L.: Quality control and flux sampling problems for tower and aircraft data, Journal of atmospheric and oceanic technology, 14, 512–526, 1997

Vickers, D., & Mahrt, L. (2004). Evaluating formulations of stable boundary layer height. *Journal of applied meteorology*, *43*(11), 1736-1749.

Wilczak, J. M., Oncley, S. P., & Stage, S. A. (2001). Sonic anemometer tilt correction algorithms. *Boundary-layer meteorology*, *99*(1), 127-150.

Zahn, E., Chor, T., and Dias, N.: A simple methodology for quality control of micrometeorological datasets, Am J Environ Eng, 6, 135–142, 2016